**PHYSICS AND CHEMISTRY OF SOLID STATE**
V. 26, No. 2 (2025) pp. 377-385
*Section: Physics*

**DOI: 10.15330/pcss.26.2.377-385**

*Vasyl Stefanyk Precarpathian National University*

**ФІЗИКА І ХІМІЯ ТВЕРДОГО ТІЛА**
**Т. 26, № 2 (2025) С. 377-385**
*Фізико-математичні науки*

PACS: 71.15.Mb; 62.20.Qp

ISSN 1729-4428 (Print)
ISSN 2309-8589 (Online)

P.M. Prysyazhnyuk[1], I.P. Yaremiy[2], A.H. Kharlov[1], M.P. Makohin[2], I.M. Umantsiv[2], V.V. Savchyn[2] and O.I. Misiuk[2]

# First-Principles Study of the Mechanical Properties of (Ti,V)C Solid Solutions

[1]*Department of Computerized Engineering, Ivano-Frankivsk National Technical University of Oil and Gas, Ivano-Frankivsk, Ukraine; pavlo.prysiazhniuk@nung.edu.ua*
[2]*Department of Applied Physics and Material Science, Vasyl Stefanyk Precarpathian National University, Ivano-Frankivsk, Ukraine*

Ternary transition metal carbides like $Ti_{1-x}V_xC$ offer potential for enhanced mechanical properties, but exploring the vast compositional space is challenging. This study employs first-principles calculations combined with the Cluster Expansion (CE) method to systematically investigate the phase stability, elastic properties, hardness, and electronic structure of the $Ti_{1-x}V_xC$ system. Density Functional Theory (DFT) calculations using VASP informed the CE model constructed via the ATAT toolkit, which predicted several stable intermediate configurations at 0 K relative to TiC and VC. Elastic constants calculated for these stable phases revealed non-monotonic trends, with Shear (G) and Young's (E) moduli peaking near x = 0.5. Vickers hardness (Hv), estimated by averaging five empirical models based on calculated Bulk (B) and G moduli, was found to reach a maximum of approximately 32.6 GPa at the $Ti_{0.67}V_{0.33}C$ composition, surpassing the calculated values for the binary endpoints. Analysis of Pugh's ratio (B/G) indicated intrinsic brittleness across all compositions, with maximum brittleness correlating with the region of maximum stiffness. Electronic structure calculations (DOS, ELF, Deformation Density) using the BAND code confirmed strong covalent p-d hybridization as the origin of the high stiffness and revealed composition-dependent changes related to Fermi level shifts. This work identifies $Ti_{0.67}V_{0.33}C$ as the most promising composition for maximizing hardness in this system and provides theoretical guidance for designing advanced carbide-based materials.

**Keywords:** Titanium vanadium carbide; density functional theory; cluster expansion; hardness prediction; electronic structure.

*Received 07 December 2024; Accepted 14 July 2025.*

## Introduction

Transition metal carbides (TMCs) form a crucial class of materials renowned for their exceptional physical and mechanical properties, including extremely high hardness, high melting points, excellent wear resistance, and good chemical stability [1]. These characteristics make them indispensable components in applications demanding high performance under extreme conditions, such as cutting tools, wear-resistant coatings, and high-temperature structural parts [2], [3]. Among the well-studied TMCs, titanium carbide (TiC) and vanadium carbide (VC) are prominent examples. Both typically crystallize in the rock-salt (NaCl) structure and exhibit high hardness (Hv ~25-30 GPa) and elastic moduli, making them technologically significant materials [4].

Alloying different transition metals within the carbide lattice offers a promising strategy for further tailoring and potentially enhancing material properties beyond those of the binary constituents. The formation of ternary solid solutions or ordered compounds can lead to effects like solid solution strengthening, modification of electronic structure, and altered phase stability, providing pathways to optimize performance for specific applications [5]. The pseudo-binary system formed by alloying TiC and VC, namely $Ti_{1-x}V_xC$, is particularly interesting for different

applications [6], [7]. Owing to their similar crystal structure and chemical nature, Ti and V exhibit significant mutual solubility and form a wide single-phase region at high temperatures (e.g., 1000°C and 1200°C) that is stable upon cooling to room temperature [8]. Exploring this ternary system could potentially yield materials with hardness or other mechanical properties superior to either binary TiC or VC or allow for fine-tuning of properties across the compositional range ($0 \leq x \leq 1$). However, despite its potential, the Ti-V-C system, particularly the detailed relationship between composition, atomic arrangement, stability, and mechanical properties, remains relatively less explored compared to some other ternary carbide systems.

Experimentally mapping the phase stability and properties across the entire compositional range of $Ti_{1-x}V_xC$ is a formidable task due to the vast number of possible atomic configurations (distributions of Ti and V on the metal sublattice) and the challenges associated with synthesizing and characterizing samples across many compositions, especially potential ordered phases which may require specific sintering and annealing conditions [9]. Computational methods based on first-principles quantum mechanics offer a powerful alternative for predicting material properties and guiding experimental efforts. DFT has emerged as a highly successful and widely used approach for accurately calculating the total energies, equilibrium structures, electronic properties, and mechanical response (e.g., elastic constants) of materials from fundamental principles. Computational investigations of refractory carbide alloys using DFT have frequently employed approaches including the Virtual Crystal Approximation (VCA), explicit supercells [10], [11], and Special Quasirandom Structures (SQS) [12]. However, these methods possess significant limitations regarding the accurate prediction of phase stability and ground-state configurations. The VCA, which averages the properties of constituent atoms, inherently neglects the crucial effects of the local chemical environment and atomic relaxations. Consequently, it often fails to capture the energetic stabilization associated with chemical ordering, leading to inaccurate formation energy predictions, particularly for potentially stable ordered compounds. On the other hand, approaches based on SQS or manually constructed supercells, while capable of modeling random solid solutions or specific configurations (supercells), do not systematically explore the vast configurational landscape. SQS assumes complete randomness by design, while supercell studies are often limited by computational cost to a small subset of possible arrangements. As a result, both methods risk overlooking the most thermodynamically stable atomic arrangements (i.e., ordered ground states or low-energy structures) within the solid solution, which possess the lowest formation energies. To overcome this limitation, the CE method provides an efficient solution [12]. The CE technique allows mapping of the configuration-dependent properties (like formation energy), calculated via DFT for a relatively small set of training structures, onto a generalized Ising-like Hamiltonian based on interactions between clusters of lattice sites (points, pairs, triplets, etc.). Once the effective cluster interactions (ECIs) are determined, the CE Hamiltonian can be used to rapidly predict the energy and other properties of arbitrary configurations, enabling efficient exploration of the entire composition and configuration space. The Alloy Theoretic Automated Toolkit (ATAT) package integrates DFT calculations (like those from VASP) with CE construction and subsequent thermodynamic or ground-state analysis, providing a powerful workflow for alloy theory [13].

In this study, we employ a synergistic approach combining first-principles DFT calculations with the CE method implemented in ATAT to systematically investigate the $Ti_{1-x}V_xC$ carbide system. Our primary objectives are: (1) To determine the ground-state phase stability across the entire composition range ($0 \leq x \leq 1$) by constructing the 0 K convex hull of formation energy. (2) To identify the crystal structures of the predicted stable and low-energy metastable phases. (3) To calculate the single-crystal and polycrystalline elastic moduli for these relevant phases using DFT. (4) To estimate the Hv based on the calculated elastic moduli using established theoretical models. (5) Ultimately, to understand the composition-property relationships and predict the optimal composition (value of 'x') in $Ti_{1-x}V_xC$ that potentially maximizes hardness, thereby providing theoretical guidance for the design and synthesis of novel high-hardness carbide materials.

# I. Calculations

All first-principles calculations were performed using the Vienna Ab initio Simulation Package (VASP) [14] within the framework of DFT. The electronic exchange and correlation effects were described using the R²SCAN meta-GGA functional [15], known for its accuracy in predicting structural and energetic properties of solids. Core and valence electrons were treated using the Projector Augmented-Wave (PAW) method [16] corresponding to the Perdew-Burke-Ernzerhof (PBE) functional were likely employed. Non-spherical contributions within the PAW spheres were for improved accuracy.

A plane-wave basis set with a kinetic energy cutoff of 600 eV was used throughout the calculations. The “Accurate” setting was enabled to ensure high precision and minimize wrap-around errors, and an additional support grid was used for the augmentation charge evaluation. The electronic Brillouin zone integration was performed using the Methfessel-Paxton first-order smearing method with a smearing width of 0.1 eV. A dense Monkhorst-Pack [17] k-point mesh was employed, generated to achieve a target density of approximately 1000 k-points per reciprocal atom (KPPRA = 1000) for all structures, ensuring convergence of total energies and stresses.

For determining the equilibrium structures used in the CE for calculating elastic constants, full structural relaxations were performed. Both atomic positions and the simulation cell shape and volume were allowed to relax using the conjugate gradient algorithm. The electronic self-consistency loop was converged to a tolerance of $1 \times 10^{-6}$ eV. The configurational energetics and phase stability within the $Ti_{1-x}V_xC$ system were modeled using maps code within the ATAT. A CE Hamiltonian,

including various cluster types, was constructed by fitting Effective Cluster Interactions (ECIs) to a database of DFT-calculated energies obtained for structures across different compositions. The predictive accuracy of the fitted Hamiltonian was assessed using the standard leave-one-out cross-validation technique. Subsequently, this CE Hamiltonian was employed to perform a ground state search over the entire concentration range ($0 \leq x \leq 1$) by evaluating candidate structures containing up to 16 atoms per unit cell, in order to identify low-energy configurations for further analysis.

For the optimized structures of end members and ground state clusters, the components of the stiffness matrix ($C_{ij}$) were calculated using VASP via the finite difference method, followed by VASPKIT analysis [18] to extract the elastic tensor. Subsequently, the effective polycrystalline B, G, E, and Poisson's ratio ($\nu$) were calculated according to the Voigt-Reuss-Hill (VRH) approximation [19] using the following formulas:

$$B = \frac{1}{9}(C_{11} + C_{22} + C_{33}) + \frac{2}{9}(C_{12} + C_{13} + C_{23}), \quad (1)$$

$$G = \frac{1}{15}(C_{11} + C_{22} + C_{33} - C_{12} - C_{13} - C_{23}) + \frac{1}{5}(C_{44} + C_{55} + C_{66}), \quad (2)$$

$$E = \frac{9GB}{G+3B}. \quad (3)$$

Next, the hardness was calculated as the average value obtained from five different methods, proposed by Teter [20], Chen [21], Tian [22], Miao [23] and Mazhnik [24] as proposed in [25].

To reveal the bonding nature of the end members (TiC and VC) and compare it to the stable cluster configurations, the Total Density of electronic states (TDOS), partial Density of electronic states (pDOS), Electron Localization Function (ELF), and Deformation Density (DD) were calculated. These analyses were performed using the BAND module within the Amsterdam Modeling Suite (AMS) software package [26]. The calculations were carried out as single point energy evaluations on the previously optimized structures. The Generalized Gradient Approximation (GGA) with the Perdew-Burke-Ernzerhof (PBE) functional was employed [27] for exchange and correlation. Scalar relativistic effects were accounted for using the Zero-Order Regular Approximation (ZORA). A triple-zeta polarized (TZP) Slater-type orbital basis set was used for all atoms, with no electrons treated within a frozen core approximation. 'Good' numerical quality setting was used, controlling aspects like integration grids.

## II. Results and discussion

The CE Hamiltonian of the pseudo-binary $Ti_{1-x}V_xC$ system at 0 K was fitted to a dataset comprising the DFT-calculated energies of 52 clusters. The predictive accuracy of the resulting CE model, quantified by the leave-one-out cross-validation (CV) score, was determined to be approximately 16.2 meV/atom. Figure 1a displays the 0 K convex hull of formation energy versus V concentration (x), as predicted by the fitted CE model. The plot includes the energies of the DFT training structures (green crosses), the CE-predicted energies for a large number of configurations (purple crosses), and the specific configurations identified by the CE as potential ground states (orange squares). The solid light-blue line represents the convex hull, connecting the lowest-energy predicted ground states at each stable composition. The convex hull clearly lies below zero formation energy for intermediate compositions, indicating that the formation of $Ti_{1-x}V_xC$ alloys or compounds is energetically favorable relative to phase separation into the binary constituents TiC (x = 0) and VC (x = 1). The presence of distinct points

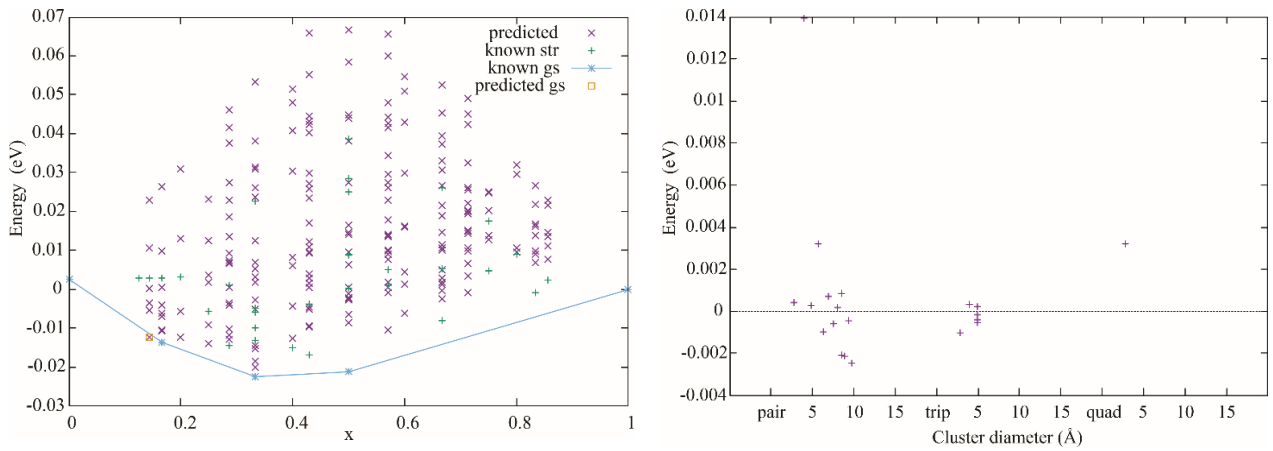


(a) (b)

**Fig. 1.** Results of CE modeling of the $Ti_{1-x}V_xC$ solid solutions (a) and fitted ECIs versus cluster diameter (Å) (b).

lying on the hull at specific compositions (e.g., x = 0.167, 0.333 and 0.5) suggests a tendency towards the formation of specific low-energy atomic configurations rather than a completely random solid solution. These represent the most probable local arrangements of atoms within the disordered alloy at low temperatures. According to this CE model, the lowest formation energy is predicted to be approximately – 0.022 eV/atom, occurring at a composition near x = 0.333. These low-energy configurations, representing the most likely stable atomic arrangements at low temperatures, were selected for further investigation as proxies for predicting the alloy's mechanical properties.

Further details of the fitted CE model are illustrated in Figure 1b, which plots the Effective Cluster Interactions (ECIs) against the corresponding cluster diameter for pairs, triplets, and quadruplets included in the expansion. The graph shows the expected physical trend where the magnitude of the ECIs generally decays rapidly with increasing cluster diameter and complexity (number of points in the cluster). This decay indicates good convergence of the expansion. The dominant interactions are primarily short-range pairs, with triplet and quadruplet terms contributing less significantly to the overall energy in this fitted model.

The calculated polycrystalline elastic moduli (Hill averages) for ground state phases and the endmembers in the $Ti_{1-x}V_xC$ system are presented as a function of composition in Figure 2. A generally increasing trend was observed for the B with increasing Vanadium content (x), although with a minor deviation near x = 0.2, reaching a maximum for VC. Conversely, the G and E exhibited distinct non-monotonic behavior, both reaching pronounced maxima at the intermediate composition x=0.5 (G~214 GPa, E~514 GPa). This peak indicates that the $Ti_{0.5}V_{0.5}C$ configuration possesses the highest calculated resistance to shear and elastic deformation among the investigated phases. The calculated shear modulus for VC (x = 1) was notably similar to that of TiC (x = 0). This finding exhibits good agreement with reported experimental values for TiC (G = 186 GPa [4]) and $VC_{0.875}$ (G = 179 GPa [28]).

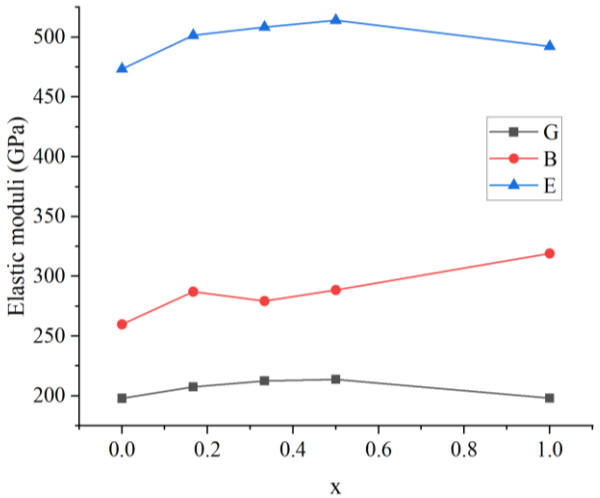


**Fig. 2.** Composition dependence of calculated polycrystalline elastic moduli (Hill averages) for calculated stable $Ti_{1-x}V_xC$ solid solutions.

Further analysis correlating mechanical indicators is shown in Figure 3, using the average Hv derived from five different empirical models [20–24]. The predicted Hv exhibits a non-monotonic trend, starting at ~30.7 GPa for TiC (x = 0), dipping slightly at x ~ 0.167, before reaching a distinct maximum value of approximately 32.6 GPa at x = 0.333. The hardness remains high at x = 0.5 (~32.0 GPa) and then decreases significantly for VC (x = 1, ~26.3 GPa). This identifies the $Ti_{0.67}V_{0.33}C$ configuration as exhibiting the highest predicted hardness based on the average of the models considered. This hardness peak occurs at a composition slightly preceding the peak observed for the shear modulus G (at x = 0.5). In contrast, Pugh's ratio [28] (B/G), an indicator of brittleness, displays an inverse relationship relative to the elastic moduli G and E, reaching its minimum (B/G ~1.35, indicating maximum brittleness) at x = 0.5, which coincides with the peak in G and E but not precisely with the peak in the averaged Hv. Nevertheless, all calculated phases fall within the brittle regime (B/G < 1.75). The Debye temperature ($\Theta_D$), reflecting lattice stiffness, also peaks at intermediate compositions (~984 K near x = 0.33), generally aligning with the region of high elastic moduli and hardness. Kleinman's parameter ($\zeta$) provides insight into bonding character, remaining relatively constant and slightly below 0.5 for TiC and intermediate phases up to x = 0.5, before increasing above 0.5 for VC. This suggests a shift towards increased importance of bond bending forces in VC, correlating with its distinct elastic response.

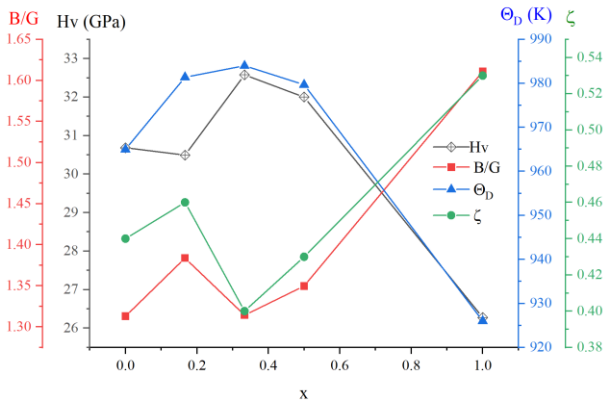


**Fig. 3.** Composition dependence of predicted Hv and Pugh's ratio, $\Theta_D$ and $\zeta$ for calculated stable $Ti_{1-x}V_xC$ solid solutions.

In summary, the combined results identify intermediate compositions as having the highest thermodynamic stability and stiffness. While the G and E moduli peak at x=0.5, the Hv, when averaged across five empirical models, is predicted to reach its maximum of ~32.6 GPa at x=0.333. This composition surpasses the calculated hardness of both binary endpoints. Although the hardest composition (x=0.333) and the most brittle composition (minimum B/G at x=0.5) do not perfectly coincide, both occur at intermediate stoichiometries where high lattice stiffness (indicated by $\Theta_D$) is also observed. These findings suggest that compositions near $Ti_{0.67}V_{0.33}C$ and $Ti_{0.5}V_{0.5}C$ are most promising for achieving high hardness in the $Ti_{1-x}V_xC$ solid solutions, although this comes with inherent brittleness.

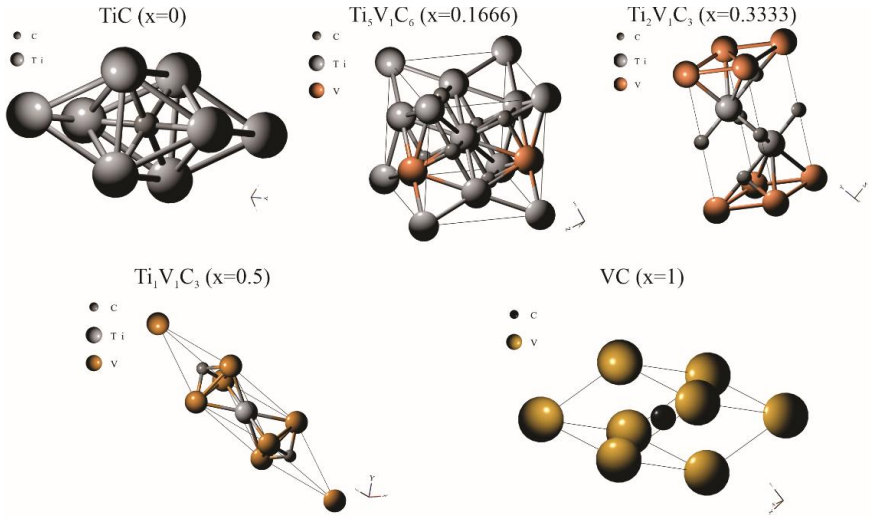


**Fig. 4.** Calculated stable crystal structures in the $Ti_{1-x}V_xC$ system for x = 0, 0.167, 0.333, 0.5, and 1.

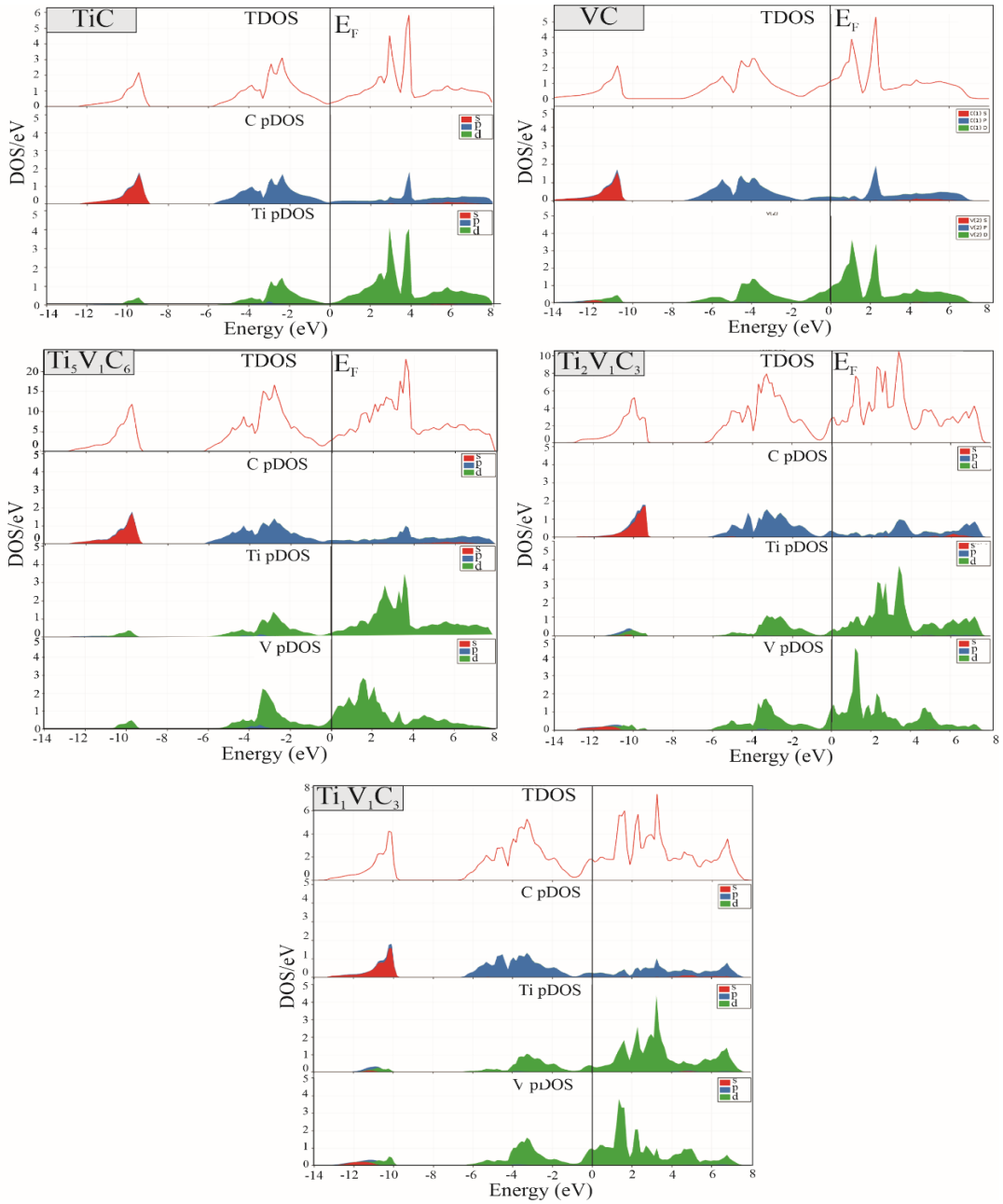


**Fig. 5.** Calculated TDOS and pDOS for TiC (x = 0), VC (x = 1), and intermediate $Ti_{1-x}V_xC$ phases (x ~ 0.333, 0.5 and 0.167). The Fermi level ($E_F$) is set to 0 eV.

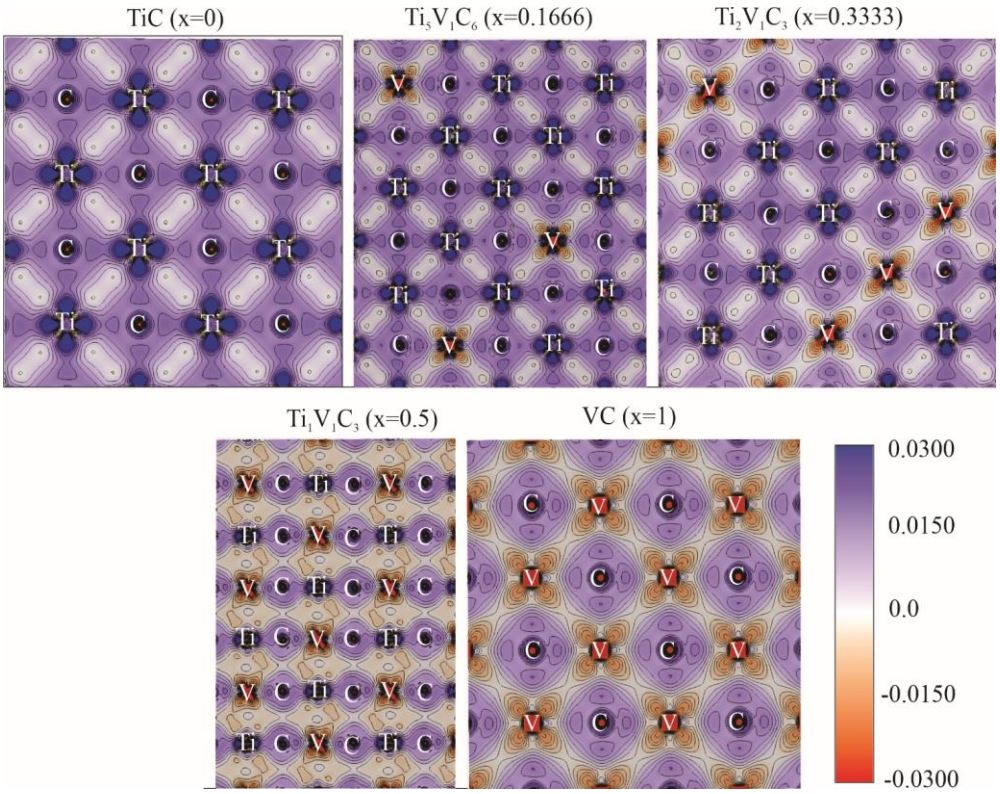


**Fig. 6.** Visualization of chemical bonding via DD (Δρ) maps for ground state $Ti_{1-x}V_xC$ structures.

To further elucidate the nature of chemical bonding driving the observed mechanical trends, the electronic structure was analyzed. The TDOS and pDOS were calculated for the key ground state configurations (crystal structures visualized in Figure 4), with the results presented in Figure 5.

Figure 5 reveals several common features across the calculated compositions. All phases exhibit metallic character, evidenced by a finite density of states at the Fermi level ($E_F$=0 eV). The valence band consists of a lower part (approximately –12 to –10 eV) dominated by C 2s states and an upper, broader part (approximately –8 eV to $E_F$) characterized by strong hybridization between C 2p states and the metal d-states (Ti 3d and/or V 3d). This p-d hybridization signifies strong covalent bonding between the metal and carbon atoms, which is fundamental to the high intrinsic stiffness and hardness of these phases. A pseudogap, or a distinct minimum in the TDOS, is observed just below $E_F$ in all cases, separating the main bonding states from the states at the Fermi level. The conduction band above $E_F$ is primarily composed of metal d-states. With increasing V concentration (x), the primary effect observed is a shift of the Fermi level to higher energies, progressively filling more states within the metal d-band complex, consistent with V contributing one more valence electron than Ti. The specific shapes and peak positions within the DOS vary with composition, reflecting the different local atomic environments and relative contributions of Ti and V d-states. The position of the Fermi level relative to the pseudogap and the degree of filling of the hybridized metal d-states are expected to strongly influence shear resistance; the peak in G and Hv near x = 0.33–0.5 suggests an optimal filling of bonding states relevant to shear deformation occurs at these intermediate compositions.

A real-space visualization of the bonding is provided by the Deformation Density (DD) maps ($\Delta\rho = \rho_{crystal} - \sum\rho_{atoms}$), presented in Figure 6 for ground state structures. In these maps, regions of charge accumulation ($\Delta\rho > 0$, blue contours) signify bond formation, while regions of charge depletion ($\Delta\rho < 0$, red contours) indicate density loss relative to isolated atoms. Across all compositions, significant charge accumulation (blue) is observed between the metal (Ti/V) and carbon atoms, providing a clear visual representation of the strong covalent character of the metal-carbon bonds arising from the p-d hybridization identified in the pDOS (Figure 5). Additionally, charge depletion (red) around the metal sites coupled with accumulation nearer the carbon sites illustrates the polar nature of these bonds, indicating charge transfer consistent with carbon's higher electronegativity. This combination of strong, directional covalent bonding and ionic contributions, visualized by the DD maps, provides a microscopic basis for the high cohesive energy and elastic stiffness (particularly the shear modulus G) calculated for these structures. Subtle variations in the intensity and spatial distribution of charge accumulation in the Ti-C versus V-C bonds, and within the different intermediate structures, likely underlie the observed non-monotonic trends in G, E, and Hv, particularly the enhancement around x = 0.5.

Further insights into electron localization and bonding type are offered by the ELF, shown in Figure 7.

ELF values range from 0 (perfect delocalization) to 1 (perfect localization). High ELF values (approaching 1.0, blue/purple regions) indicate areas where electrons are highly localized, typical of covalent bonds or lone pairs, while low values (red/orange regions) signify more delocalized, metallic-like electron distributions. Consistent with the pDOS and DD analyses, the ELF maps

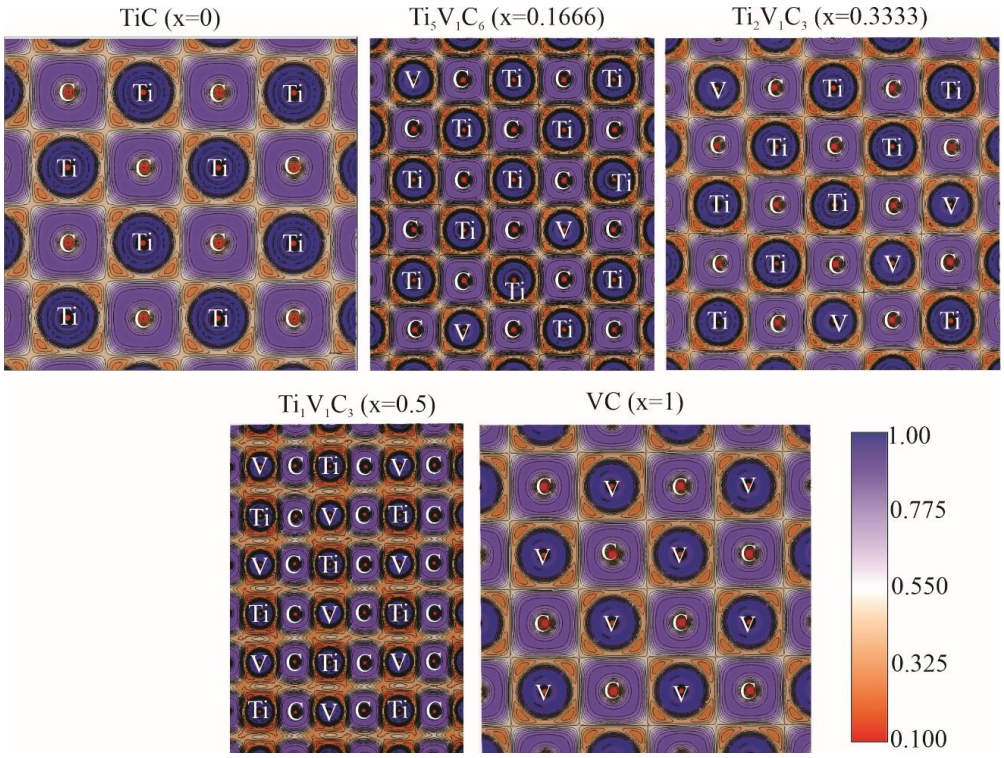


**Fig. 7.** Visualization of chemical bonding via ELF maps for ground state $Ti_{1-x}V_xC$ structures.

clearly show high localization around the carbon atoms, extending directionally towards the neighboring metal (Ti/V) atoms. This high ELF concentration in the metal–carbon bonding region is a direct signature of the strong covalent bonds formed through p-d hybridization. Conversely, the regions around the metal atoms exhibit lower ELF values, characteristic of more delocalized metallic states and consistent with the charge depletion observed in the DD maps. The interstitial regions also show low ELF values. This spatial distribution of localized electron density in the strong, directional metal–carbon bonds provides a fundamental explanation for the material's high resistance to shear deformation, contributing significantly to the calculated high G and Hv, especially for the intermediate compositions where G peaks.

## Conclusions

In this study, the phase stability, mechanical properties, and electronic structure of the $Ti_{1-x}V_xC$ system were systematically investigated using a combination of first-principles (DFT) calculations and the CE method. The CE approach successfully modeled the energetics of the system, revealing a preference for specific low-energy configurations at intermediate compositions over random solid solutions at 0 K, with ground state structures near $x = 0.33$ and $x = 0.5$ showing high thermodynamic stability relative to TiC and VC. Calculation of elastic properties for these stable configurations demonstrated non-monotonic trends with composition. While the B generally increased with V content, the G and E moduli peaked significantly at $x = 0.5$. Consequently, the predicted Hv, averaged from five empirical models, reached a maximum value of approximately 32.6 GPa for the $Ti_{0.67}V_{0.33}C$ configuration, exceeding the calculated hardness of the binary carbides. This peak hardness correlates with high shear resistance but occurs in a compositional region also associated with high predicted brittleness (minimum B/G ratio near x=0.5). Analysis of the electronic structure (DOS, DD, ELF) confirmed the presence of strong covalent Ti/V–C bonds arising from p-d hybridization, which governs the mechanical response, and illustrated how the Fermi level shift influences properties across the composition range. These findings highlight the potential for optimizing the hardness of TiVC carbides through compositional tuning, identifying compositions near $x = 0.33–0.5$ as the most promising targets, and provide valuable theoretical data to guide future experimental synthesis and characterization efforts.

**Acknowledgements**

The authors wish to express their sincere gratitude and respect to the Armed Forces of Ukraine, whose resilience and defense made this work possible. This research was supported by the Ministry of Science and Education of Ukraine under grant No. 0123U101858.

***Prysyazhnyuk P.M.*** – Doctor of Technical Sciences, Associate Professor;
***Yaremiy I.P.*** – Doctor of Physical and Mathematical Sciences, Professor;
***Kharlov A.*** – Ph.D. student;
***Makohin M.P.*** – Ph.D. student;
***Umantsiv I.M.*** – Ph.D. student;
***Savchyn V.V.*** – Ph.D. student;
***Misiuk O. I.*** – Ph.D. student.

[1] T. Qin, Z. Wang, Y. Wang, F. Besenbacher, M. Otyepka, and M. Dong, *Recent Progress in Emerging Two-Dimensional Transition Metal Carbides References,* Nano-Micro Lett. 13, 143 (2021); https://doi.org/10.1007/s40820-021-00710-7.
[2] P. Prysyazhnyuk, O. Ivanov, O. Matvienkiv, S. Marynenko, O. Korol, and I. Koval, *Impact and abrasion wear resistance of the hardfacings based on high-manganese steel reinforced with multicomponent carbides of Ti-Nb-Mo-V-C system*, Procedia Struct. Integr. 36, 130 (2022); https://doi.org/10.1016/j.prostr.2022.01.014.
[3] S. T. A. Shihab, P. Prysyazhnyuk, R. Andrusyshyn, L. Lutsak, O. Ivanov, and I. Tsap, *Forming the structure and the properties of electric arc coatings based on high manganese steel alloyed with titanium and niobium carbides*, East.-Eur. J. Enterp. Technol. 1, 38 (2020); https://doi.org/10.15587/1729-4061.2020.194164.
[4] M. Mhadhbi, *Titanium Carbide: Synthesis, Properties and Applications*, Brilliant Eng. 2, 1 (2020); https://doi.org/10.36937/ben.2021.002.001.
[5] L. Trinh et al., J. Am., Selective laser sintering and spark plasma sintering of *(Zr,Nb,Ta,Ti,W)C compositionally complex carbide ceramics*, Ceram. Soc. 107, 7175 (2024); https://doi.org/10.1111/jace.20019.
[6] W. Wei, X. Ying, W. Xu, H. Zhiquan, and L. Shengxin, *Effect of V content on microstructures and properties of TiC cermet fusion welding interface*, China Weld. 33, 40 (2024); https://doi.org/10.12073/j.cw.20231212019.
[7] M. Chen et al., *Effect of VC addition on the microstructure and properties of TiC steel-bonded carbides fabricated by two-step sintering*, Int. J. Refract. Met. Hard Mater. 108, 105948 (2022); https://doi.org/10.1016/j.ijrmhm.2022.105948.
[8] R. Picha, A. Kroupa, and P. Broz, *Phase Diagram of the Ti-V-C System at 1000 and 1200° C*, Arch. Metall. Mater. No 2, 139 (2001).
[9] M. Chen, X. Zhang, X. Xiao, and H. Zhao, *Effect of VC additions on the microstructure and mechanical properties of TiC-based cermets,* Mater. Res. Express 7, 106527 (2020); https://doi.org/10.1088/2053-1591/abc2a1.
[10] Q. Wang, Q. Li, H. Ding, and F. Tian, *Elastic properties of solid-solution refractory metal carbides with vacancy from virtual crystal approximation and supercell method*, Comput. Condens. Matter 32, e00721 (2022); https://doi.org/10.1016/j.cocom.2022.e00721.
[11] P. Prysyazhnyuk et al., *Analysis of the effects of alloying with Si and Cr on the properties of manganese austenite based on AB INITIO modelling*, East.-Eur. J. Enterp. Technol. 6, 28 (2020); https://doi.org/10.15587/1729-4061.2020.217281.
[12] J. Kim, *First-principles investigation of the elastic properties and phase stability of (Ti1-xNix)C1-y ternary metastable carbides*, J. Alloys Compd. 853, 157349 (2021); https://doi.org/10.1016/j.jallcom.2020.157349.
[13] A. van de Walle, M. Asta, and G. Ceder, *The alloy theoretic automated toolkit: A user guide*, Calphad 26, 539 (2002); https://doi.org/10.1016/s0364-5916(02)80006-2.
[14] J. Hafner and G. Kresse, *The Vienna AB-Initio Simulation Program VASP: An Efficient and Versatile Tool for Studying the Structura*l, Dynamic, and Electronic Properties of Materials, in Properties of Complex Inorganic Solids (Springer US, 1997) pp. 69–82; https://doi.org/10.1007/978-1-4615-5943-6_10.
[15] J. W. Furness, A. D. Kaplan, J. Ning, J. P. Perdew, and J. Sun, *Accurate and Numerically Efficient r2SCAN Meta-Generalized Gradient Approximation*, J. Phys. Chem. Lett. 11, 8208 (2020); https://doi.org/10.1021/acs.jpclett.0c02405.
[16] G. Kresse and D. Joubert, *From ultrasoft pseudopotentials to the projector augmented-wave method*, Phys. Rev. B 59, 1758 (1999); https://doi.org/10.1103/physrevb.59.1758.
[17] H. J. Monkhorst and J. D. Pack, *Special points for Brillouin-zone integrations*, Phys. Rev. B 13, 5188 (1976); https://doi.org/10.1103/PhysRevB.13.5188.
[18] V. Wang, N. Xu, J.-C. Liu, G. Tang, and W.-T. Geng, *VASPKIT: A user-friendly interface facilitating high-throughput computing and analysis using VASP code,* Comput. Phys. Commun. 267, 108033 (2021); https://doi.org/10.1016/j.cpc.2021.108033.
[19] R. Hill, *The Elastic Behaviour of a Crystalline Aggregate*, Proc. Phys. Soc. A 65, 349 (1952); https://doi.org/10.1088/0370-1298/65/5/307.
[20] *D. M. Teter, Computational alchemy: The search for new superhard materials*, MRS Bull. 23, 22 (1998); https://doi.org/10.1557/S0883769400031420.
[21] X.-Q. Chen, H. Niu, D. Li, and Y. Li, *Modeling hardness of polycrystalline materials and bulk metallic glasses*, Intermetallics 19, 1275 (2011); https://doi.org/10.1016/j.intermet.2011.03.026.
[22] Y. Tian, B. Xu, and Z. Zhao, *Microscopic theory of hardness and design of novel superhard crystals*, Int. J. Refract. Met. Hard Mater. 33, 93 (2012); https://doi.org/10.1016/j.ijrmhm.2012.02.021.
[23] N. Miao, B. Sa, J. Zhou, and Z. Sun, *Theoretical investigation on the transition-metal borides with Ta3B4-type structure: A class of hard and refractory materials*, Comput. Mater. Sci. 50, 1559 (2011); https://doi.org/10.1016/j.commatsci.2010.12.015.
[24] E. Mazhnik and A. R. Oganov, *A model of hardness and fracture toughness of solids*, J. Appl. Phys. 126, 125109 (2019); https://doi.org/10.1063/1.5113622.
[25] P. Prysyazhnyuk and D. Di Tommaso, *The thermodynamic and mechanical properties of Earth-abundant metal ternary boride $Mo_2(Fe,Mn)B_2$ solid solutions for impact- and wear-resistant alloys*, Mater. Adv. 4, 3822 (2023); https://doi.org/10.1039/D3MA00313B.
[26] G. te Velde and E. J. Baerends, *Precise density-functional method for periodic structures*, Phys. Rev. B 44, 7888 (1991); https://doi.org/10.1103/PhysRevB.44.7888.

[27] J. P. Perdew, K. Burke, and M. Ernzerhof, *Generalized Gradient Approximation Made Simple*, Phys. Rev. Lett. 77, 3865 (1996); https://doi.org/10.1103/PhysRevLett.77.3865.
[28] X. Zhang, J.D. Comins, A.G. Every and P.R. Stoddart, *Surface Brillouin scattering studies on vanadium carbide*, Int. J. Refract. Met. Hard Mater. 16, 303 (1998); https://doi.org/10.1016/S0263-4368(98)00046-8.
[29] S. F. Pugh, *XCII. Relations between the elastic moduli and the plastic properties of polycrystalline pure metals*, Philos. Mag. 45, 823 (1954); https://doi.org/10.1080/14786440808520496.

П. М. Присяжнюк[1], І. П. Яремій[2], А. Г. Харлов[1], М. П. Макогін[2], І. М. Уманців[2], В. В.Савчин[2], О. І. Місюк[2]

# Першопринципний аналіз механічних властивостей твердих розчинів (Ti,V)C

*[1]Кафедра комп'ютеризованої інженерії, Івано-Франківський національний технічний університет нафти і газу, Івано-Франківськ, Україна; pavlo.prysiazhniuk@nung.edu.ua,*
*[2]Кафедра прикладної фізики та матеріалознавства, Прикарпатський національний університет імені Василя Стефаника, Івано-Франківськ, Україна*

Потрійні карбіди перехідних металів, такі як $Ti_{1-x}V_xC$, мають потенціал для покращення механічних властивостей, але дослідження широкого композиційного простору є складним завданням. У цьому дослідженні застосовуються першопринципні розрахунки в поєднанні з методом кластерного розширення (CE) для систематичного вивчення фазової стабільності, пружних властивостей, твердості та електронної структури системи $Ti_{1-x}V_xC$. Розрахунки за теорією функціоналу густини (DFT) з використанням пакета VASP лягли в основу моделі (CE), побудованої за допомогою інструментарію програми ATAT, яка передбачила кілька стабільних проміжних конфігурацій при 0 K відносно TiC та VC. Пружні сталі, розраховані для цих стабільних фаз, продемонстрували немонотонні тенденції, при цьому модулі зсуву (G) та Юнга (E) досягали пікових значень поблизу x = 0.5. Було встановлено, що твердість за Віккерсом (Hv), оцінена шляхом усереднення п'яти емпіричних моделей на основі розрахованих модулів всебічного стиску (B) та зсуву (G), досягає максимуму приблизно 32.6 ГПа при складі $Ti_{0.67}V_{0.33}C$, перевищуючи розрахункові значення для бінарних кінцевих сполук. Аналіз коефіцієнта П'ю (B/G) вказав на крихкість для усіх складів, причому максимальна крихкість корелювала з областю максимальної жорсткості. Розрахунки електронної структури (густина електронних станів, функція локалізації електронів, деформаційна густина) з використанням коду BAND підтвердили сильну ковалентну p-d гібридизацію як причину високої жорсткості та виявили залежні від складу зміни, пов'язані зі зміщенням рівня Фермі. Ця робота визначає $Ti_{0.67}V_{0.33}C$ як найбільш перспективний склад для максимізації твердості в цій системі та надає теоретичні орієнтири для розробки нових матеріалів на основі карбідів.

**Ключові слова:** карбід титану-ванадію; теорія функціоналу густини; кластерне розширення; прогнозування твердості; електронна структура.